Songklanakarin J. Sci. Technol.
43 (1), 96-104, Jan. - Feb. 2021

http://www.sjst.psu.ac.th

Original Article

Experimental studies and artificial neural network modeling of hydrogen sulfide removal from wastewater by calcium-modified coconut shell based activated carbon

Omar Abed Habeeb[1, 2], Bamidele Victor Ayodele[3*], May Ali Alsaffar[4], Tuan Ab Rashid Bin Tuan Abdullah[3], Ramesh Kanthasamy[5], and Rosli Bin Mohd. Yunus[1]

[1] *Faculty of Chemical and Process Engineering Technology, College of Engineering Technology, Universiti Malaysia Pahang, Gambang, Pahang, 26300 Malaysia*

[2] *North Refinery Company, Ministry of Oil, Salah Aldeen, Baiji, Iraq*

[3] *Institute of Energy Policy and Research, Universiti Tenaga Nasional, Kajang, Selangor, 43000 Malaysia*

[4] *University of Technology, Baghdad, Iraq*

[5] *King Abdulaziz University, Rabigh Branch, Jeddah, Saudi Arabia*

Received: 4 April 2019; Revised: 19 July 2019; Accepted: 12 November 2019

Abstract

In this study, activated carbon -based adsorbent was prepared from eggshells and coconut shells. The effects of contact time, initial H_2S concentration, and the calcium impregnated coconut shell activated carbon (Ca-CSAC) adsorption dosage on the hydrogen sulphide (H_2S) removal efficiency and adsorption capacity were investigated. The batch adsorption data obtained from the experimental runs were employed to fit an artificial neural network (ANN) model. An initial optimization was performed to obtain the most suitable number of hidden neurons for training and validation of the ANN. The optimization results show that 16 hidden neurons was the most appropriate choice. The trained ANN was adequately validated and tested with coefficients of determination (R^2) of 0.99 and 0.95, respectively. The ANN was found to be a robust tool for modeling of H_2S removal efficiency by and adsorption capacity on Ca-CSAC under different process conditions.

Keywords: artificial neural network, adsorbent, hydrogen sulfide, coconut shell, modelling

1. Introduction

The refining of crude oil to obtain different fractions of petroleum products is often accompanied with negative environmental impacts from the release of pollutants, such as hydrogen sulphide (H_2S) usually present in the discharged process wastewater (Elmawgoud, Elshiekh, Khalil, Alsabagh, & Tawfik, 2015). The presence of H_2S in process water is a potential health risk and often results in significant economic losses arising from the fouling of the resin bed and the corrosion of process equipment (Strahand, 2010). In order to mitigate these economic losses and negative environmental impacts, prior studies have sought to develop state-of-the-art techniques for the removal of this toxic gas pollutant (Guerrero *et al.*, 2016).

*Corresponding author
Email address: ayodelebv@gmail.com;
omer_habeeb2003@yahoo.com

Physicochemical techniques such as air stripping (Al-Haddad, Azrag, & Mukhopadhyay, 2014), catalytic oxidation (Kastner, Das, Buquoi, & Melear, 2003), the use of ferric/alum water treatment residuals (Wang & Pei, 2012) and adsorption (Xiao, Wang, Wu, & Yuan, 2008) have been employed for the removal of this toxic pollutant from process waters. In comparison to other methods, adsorption as the separation process has gained wide acceptance as a technique for purifying wastewater on an industrial scale by using porous media such as activated carbon (Seredych & Bandosz, 2011). The discovery of using porous media by McBain (1932) for the adsorption of vapours in large quantities can be dated to 1932. However, its industrial applications to wastewater treatment span only a few decades due to some advances made. The use of activated carbons to remove toxic H_2S is gaining wide acceptance due to several benefits, such as large savings in energy costs, low operating costs, and comparatively small equipment size (Mailler *et al.*, 2016). Besides, activated carbons possess excellent physicochemical properties, such as large surface area, microporosity, and good surface chemistry, which have made them the most sought after medium for removing toxic pollutants from refinery effluents (Dias *et al.* 2007; Ioannidou & Zabaniotou 2007). However, commercially available activated carbon is not cost effective, motivating the quest for low-cost sources of activated carbons from locally available materials (Ioannidou & Zabaniotou 2007).

Several authors have investigated the use of activated carbon for the removal of toxic substances from water, by using coconut shell (Bagreev, Rahman, & Bandosz, 2000), palm kernel shell (Guo *et al.*, 2007), wood, and lignite (Adib, Bagreev, & Bandosz, 1999). All the aforementioned studies focused on the adsorption capacity and kinetic modeling of the H_2S removal from wastewater. To the best of the authors' knowledge, there is no prior published study on predictive models for H_2S removal from wastewater using calcium (Ca) modified coconut shell activated carbon. The main objective of this study was to investigate the effects of process parameters, such as adsorption contact time, initial H_2S concentration and adsorbent dosage on the H_2S removal efficiency and on the adsorption capacity of Ca-CSAC; as well as developing an artificial neural network model that can predict the H_2S removal efficiency and the adsorption capacity of the Ca-modified coconut shell -based activated carbon. The application of ANN in predictive modelling of the adsorption process will facilitate dealing with the non-linear relationships between the input and the output variables. This will enhance setting the process variables for optimum performance.

2. Materials and Methods

2.1 Preparation of adsorbent

The coconut shell waste residue (CNS) used in this study was collected from a commercial farm located close to the Universiti Malaysia Pahang (UMP), Gambang, Pahang, Malaysia. The collected CNS was washed with distilled water to remove soil and other impurities. Thereafter, the CNS was dried in the sun and subsequently ground and sieved to particle sizes of 0.5-1 mm. In order to ensure that the ground CNS is free from moisture, it was further dried in an oven at 110 ^oC for 24 h. After drying, the CNS precursor was mixed with KOH at optimum KOH/precursor ratio of 4:1 as stipulated by Cazetta *et al.* (2011) and left in a mechanical shaker for proper mixing. After 24 h of mixing, the slurry was filtered and placed in a tubular horizontal reactor for treatment with N_2. The reactor temperature was increased from room temperature to 750 ^oC in order to gradually heat the slurry for contact activation time of 120 min. The gas was thereafter switched to CO_2 for an additional 2 h. The resulting activated carbon formed from the heat treatment was washed using boiled aqueous solution of HCl for 1 h in order to neutralize the KOH. This was followed by washing the activated carbon with distilled water until a neutral pH was attained. The final activated carbon products were dried at 110 °C for 24 h in order to remove any traces of moisture, and are here labeled as coconut shell activated carbon (CSAC)

The eggshells used as a source of calcium were obtained from poultry waste disposal Centre at Kajang-Malaysia. The eggshells were washed to remove dirt and other traces of impurities. After washing, the eggshells were dried, blended, and sieved using a sieve to a diameter range of 0.25-0.5mm. The powdery form of the eggshell was further dried at 105 ^oC for 8 h and thereafter soaked in acetic acid solution (25-75 vol. %) for 48 h in order to extract the calcium. The Ca solution to be impregnated into the adsorbent was prepared by mixing 0.2 g of the powdered eggshell per ml of acetic acid. The mixing was performed under constant stirring (150 rpm) at 30 °C for 2 h. Subsequently, the slurry obtained was evaporated at 66 °C and thereafter dried at 100 °C for 15 h. Finally, the Ca-impregnated carbon was further heat-treated and then washed with deionized water at 50 °C until neutral pH of adsorbent was obtained. The final Ca-impregnated adsorbent was finally dried at 100 °C for 24 h. The pyrolyzed Ca-CSAC was stored in a sealed flask and kept in a desiccator prior to the adsorption study.

2.2 Adsorbent characterization

Scanning electron microscopy (SEM) (HITACHI S-3400N system) was employed for investigating the textural morphologies of the Ca-CSAC**.** The textural properties of the activated carbon were measured by N_2 adsorption-desorption isotherms at −196 using an ASAP 2010 apparatus (Micromeritics Co., USA). Brunauer–Emmett–Teller (BET) and Barrett-Joyner-Halenda (BJH) methods were used to estimate the specific surface area (SBET, $m^2\ g^{-1}$) and total pore volume (V_t, $cm^3\ g^{-1}$ at STP) of the adsorbent. The actual density (ρ_s) of the sample was measured using helium displacement method (AccuPyc 1330 pycnometer, Micromeritics Co., USA). The pH of the carbon surface was measured by the addition of 0.4 g of dry carbon powder to 20 mL of water, followed by stirring the suspension overnight for attaining equilibrium. Elemental composition of the activated carbon was analyzed using energy-dispersive X-ray spectroscopy (EDX).

2.3 Formulation of H_2S-contaminated wastewater solution

In this study, synthetic wastewater was prepared according to the procedure reported by Asaoka *et al.* (2009a). First, a known amount of $Na_2S{\cdot}9H_2O$ was dissolved in a 500

mL solution of 0.01 M KCl purged with N_2. Second, the pH of the solution was adjusted to neutral using 0.2 M HCl (Asaoka, Yamamoto, Kondo, & Hayakawa, 2009a). H_2S can exist in solution in three forms: H_2S, bisulfide (HS^-), and sulfide (S^{2-}) (Silva, Ponte, Ponte, & Kaminari, 2011).

2.4 ANN data acquisition via batch equilibrium studies

The dataset employed in ANN modeling was obtained using batch mode experimental runs for the adsorption of H_2S. To measure the adsorption capacity and the H_2S removal efficiency, 0.1 g of the Ca-CSAC adsorbent was used in each run after degassing at 105 °C for 24 h in an oven. Batch adsorption experiments were conducted in a set of 250 mL Erlenmeyer flasks containing 100 mL of H_2S solution at various initial concentrations (100, 200, 300, 400, and 500 mg L^{-1}). The flasks were agitated in a thermostatic orbital shaker at 150 rpm and 30 °C until the equilibrium was reached. The pH of the solution was controlled to neutral by using NaOH oHCl. The adsorption capacity of the pollutants was calculated by Equation (1). Subsequently, the initial and final concentrations were measured after the suspensions were filtered.

$$q_e = \frac{(C_0 - C_e)V}{m} \quad (1)$$

where V is volume (L), m is amount of adsorbent (g), C_o and C_e are the initial and final concentrations of H_2S, respectively, and (q_e) is adsorption capacity (mg g^{-1}). The experiment was performed in a fume hood as H_2S is a very poisonous gas. Equation (2) was employed for calculating the H_2S removal efficiency.

$$\text{Removal effeciency} = \frac{C_0 - C_e}{C_0} X100 \quad (2)$$

2.5 Artificial neural network modeling

The ANN was employed to fit a non-linear model consisting of input, hidden (with weight and bias) and output layers, using the neural networks toolbox in MATLAB software environment (Joo, Yoon, Kim, Lee, & Yoon, 2015). The input parameters of the ANN are the initial H_2S concentration (100-500 mg/l), adsorption contact time (360-720min) and adsorbent dosage (0.1-1 g), while the outputs are the adsorption capacity and the H_2S removal efficiency, as shown in Figure 1. The hidden neurons between the input and output layers are scaled within the range from -1 to 1 by using hyperbolic tangent activation functions, see Equation (3). The ways the neurons are linked to each other significantly influence the performance of ANN. In the present study, the input parameters subjected to summing mechanism of the next neuron, with a view to choosing the highest probability for the output (Agatonovic-Kustrin & Beresford, 2000). Each input exemplar (data record for one experiment) is assigned a weight, which is iteratively adjusted to minimize the training error. The ANN model was of feed-forward type, which has been widely applied in industrial processes (Scott, Coveney, Kilner, Rossiny, & Alford, 2007). In addition, the feed-forward configuration is easy to implement in a variety of chemical processes. The feedforward ANN was trained using the Levenberg-Marquardt optimization algorithm (Equation (4)). The training was performed by inputting a "training data set to the ANN network" (Scott *et al.*, 2007). During the training, the ANN matches the input and output values by minimizing the difference between the predicted and the targeted values (Agatonovic-Kustrin & Beresford, 2000) by adjusting the network's interconnection weights to reduce the prediction errors iteratively. The difference between the target and the model output was quantified using the MSE defined in Equation (5) (Zamaniyan, Joda, Behroozsarand, & Ebrahimi, 2013). The ANN training and modeling were performed using the neural network toolbox in MATLAB computing environment (The Mathworks, Inc. ver.2010 a)

$$F(n) = \frac{2}{1+e^{-2n}} - 1 \quad (3)$$

where n is the number of neurons.

$$(J^t J + \lambda I)\delta = J^t \in \quad (4)$$

where J is the Jacobian matrix for the process, λ is the Levenbrg's damping factor, δ is the weight update vector and E is the output vector.

$$MSE = \frac{1}{N}\sum_{i=1}^{N}(X_i - Y_i)^2 \quad (5)$$

where N, X_i and Y_i are the number of data records in network training, the targeted output and the model output, respectively.

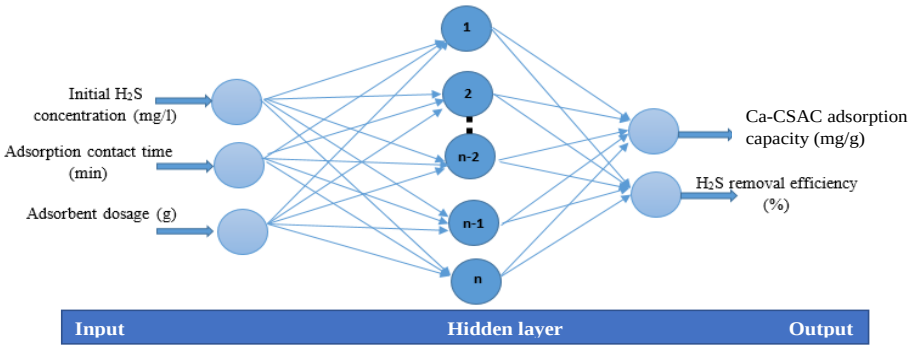

Figure 1. ANN architecture for the modeling of H_2S removal and adsorption capacity.

3. Results and Discussion

3.1 Characterization of the Ca-modified coconut shell adsorbent

The SEM is a useful technique for assessing the morphology of an adsorbent such as activated carbon. Figures 2 (a) and (b) respectively show the SEM images of the fresh coconut-based activated carbon impregnated with calcium (Ca-CSAC) (before the adsorption process) and a spent one. From Figure 2 (a), the activation with KOH helps in the formation of well-distributed pores in the activated carbon, which invariably facilitates the adsorption of sulfur compounds. In comparison with the used Ca-CSAC, the SEM image in Figure 2 (b) shows the possibility of the blockages of the pores in Ca-CSAC due to the adsorption of sulfur compounds. The adsorption of sulfur compounds can further be corroborated by the presence of a white-appearing particles on the surface of the adsorbent, seen in Figure 2 (b).

EDX micrographs showing the elemental compositions of the fresh and the used Ca-CSAC are shown in Figure 2 a and b, respectively. It can be seen from the EDX micrograph that the fresh Ca-CSAC had mainly C, Ca, K, and O. The presence of a metal such as calcium has been found to enhance the adsorption capacity of the adsorbent (Wang *et al.*, 2016). This elemental make-up of the Ca-CSAC is consistent with that reported by Cazetta *et al.* (2011). On the other hand, the used Ca-CNSAC has S in addition to C, Ca K and O which implies the removal of sulfur from the simulated wastewater. The compositional analyses of fresh and used Ca-CSAC are presented in Table 1. The EDX also shows a slight decrease in the amounts of C, Ca, K and O, possibly due to the partial blockage of the pores by the adsorbed sulfur compound.

Table 1. Elemental compositions of the fresh and the used coconut shell -based adsorbent obtained from EDX analysis.

Element	Component of fresh adsorbent (Weight %)	Components of spent adsorbent (Weight %)
Carbon (C)	88.639	83.16
Oxygen (O)	9.156	13.02
Potassium (K)	0.916	0.029
Calcium (Ca)	1.289	0.543
Sulfur (S)	0.000	3.241

The BET specific surface of the fresh Ca-CSAC adsorbent was estimated as 582 m^2/g with a corresponding pore volume and average pore diameter of 0.33 cm^3/g and 3.547 nm, respectively. These values are typical of a mesoporous material as indicated by Gupta *et al.* (2011). The BET surface area of 582 m^2/g obtained for the fresh Ca-CNSAC is smaller than the 783 m^2/g reported by Cazetta *et al.* (2011) for NaOH-modified coconut shell-based activated carbon. The difference in the BET surface areas of the two coconut shell -based adsorbents could be from effects of modification with Ca and NaOH. Nevertheless, the large surface area obtained for the fresh Ca-CNSAC is beneficial for the removal of sulphur compounds from wastewater.

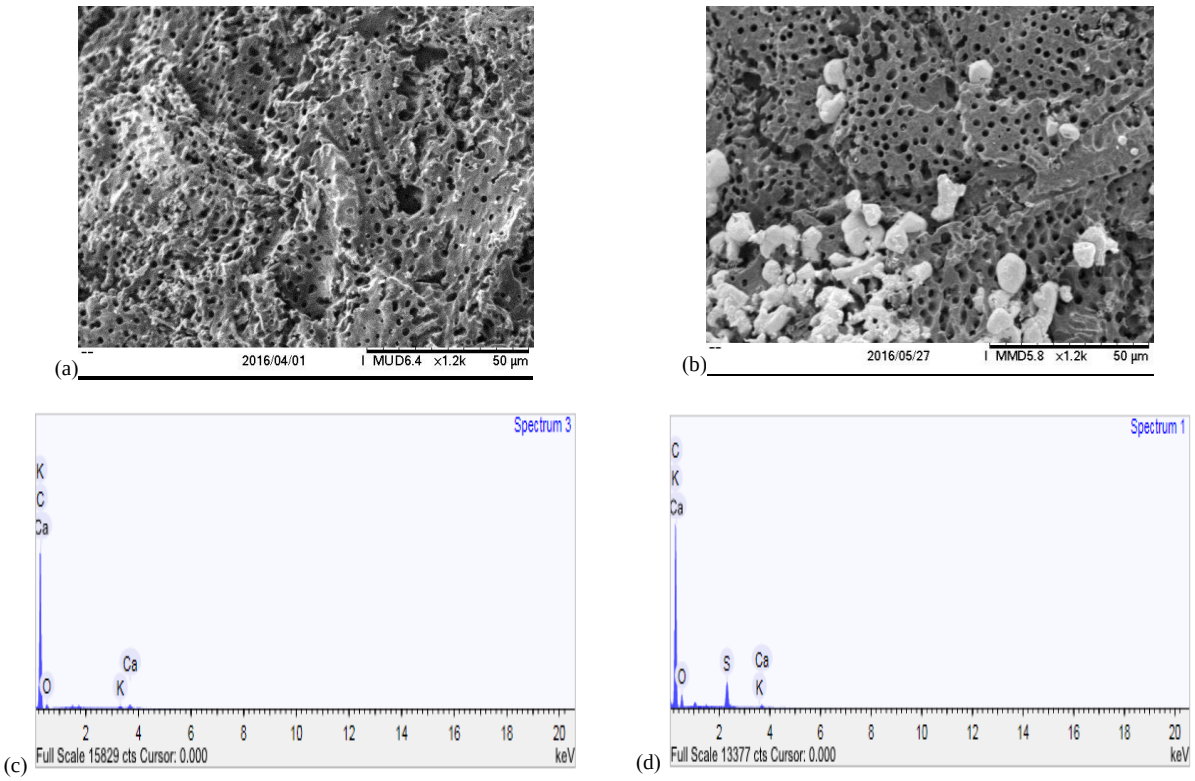

Figure.2. (a) SEM image of the fresh Ca-CSAC adsorbent, (b) SEM image of the used Ca-CSAC, (c) EDX micrograph of the fresh Ca-CSAC adsorbent, and (d) EDX micrograph of the used Ca-CSAC adsorbent

The XRD pattern showing the crystallinity of the Ca-CNSAC adsorbent is seen in Figure 3. Interestingly, various diffraction peaks signifying components of the as-prepared Ca-CNSAC can be identified. The diffraction peaks at 2θ = 29.84 º, 36.97 º, 39.89 º, 47.59 º, 57.79 º, 61.11 º, 61.77 º, 65.98 º, 69.62 º, 70.52 º, 73.26 º, 76.65 º and 77.5 º can be attributed to cubic CS_2, as evidence of the adsorption of sulfide onto the surface of the Ca-CSAC adsorbent. In addition, the diffraction peaks at 2θ = 23.53 º, 26.93º, 31.87º, 36.44º, and 77.55º could be due to cubic Ca, which confirms the presence of Ca in the adsorbent. The unused active sites of the coconut -based activated carbon are confirmed by the diffraction peak at 2θ = 43.63 º.

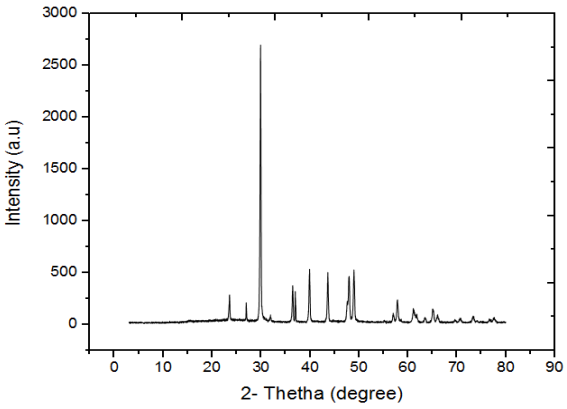

Figure 3. XRD pattern of the Ca-CSAC adsorbent

3.2 Effects of process parameters on the adsorption capacity of and removal efficiency by Ca-CSAC

Prior to the neural network modeling, the effects of initial H_2S concentration, adsorption contact time and adsorbent dosage on the adsorption capacity and removal efficiency of the Ca-CSAC were investigated. Figure 4 shows 3-D plots of the effects of the various parameters on the adsorption capacity and H_2S removal efficiency of the Ca-CSAC adsorbent. From Figures 4 (a) and (b), it can be seen that the initial H_2S concentration, the adsorption contact time and the adsorbent dosage have varying effects on the adsorption capacity of the Ca-CSAC adsorbent. In Figure 4 (a), increasing adsorption contact time from 100 to 500 min resulted in a corresponding increase in the absorption capacity from 60 to 320 mg/g. A similar trend is also observed when increasing the initial ion concentration. However, varying the adsorbent dosage does not significantly impact the adsorption capacity. In Figures 4 (c) and (d), the H_2S removal efficiency was found to increase with adsorption contact time, initial H_2S concentration, and adsorbent dosage. The interactions between ad-

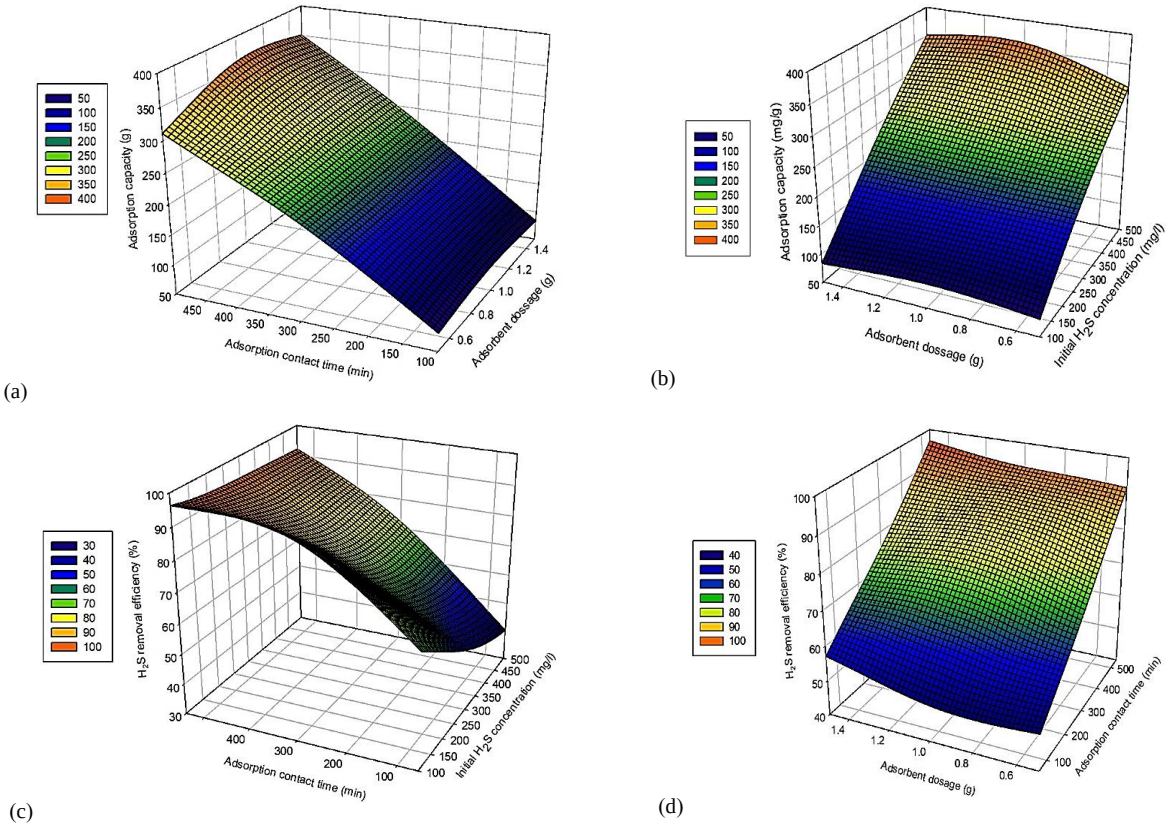

Figure 4. The effects of (a) contact time and initial H_2S conc. on the adsorption capacity, (b) adsorption dosage and initial H_2S conc. on the adsorption capacity, (c) contact time and initial H_2S conc. on the removal efficiency, and (d) adsorption dosage and initial H_2S conc. on the H_2S removal efficiency

sorption contact time, initial H_2S concentration, and adsorbent dosage gave the maximum H_2S removal efficiency of 95%. It can be seen that the various parameters have synergistic effects on the adsorption capacity and the H_2S removal efficiency rather than mutually independent effects.

3.3 Artificial neural network modeling

Prior to the neural network modeling, the hidden layer of the neural network was optimized in order to obtain the least mean standard error (MSE). Based on the optimization (Figure 5), it was noted that too few hidden neurons gave a large MSE. However, when the higher hidden layer was chosen appropriately, lower values of MSE were obtained. Hence, 14 hidden neurons were selected for the neural network modeling, which is consistent with that reported by Khataee, & Khani (2009).

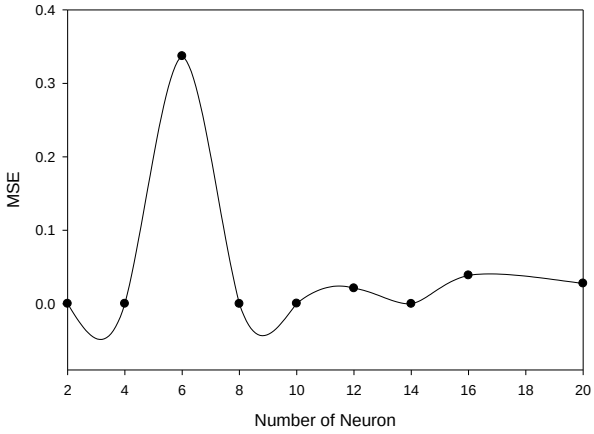

Figure 5. Optimization of the hidden layer size, based on MSE

Subsequently, the data from batch runs were employed to train and validate the neural network using 16 hidden neurons. The training of the neural network was done using 70% of the data as prescribed by Ayodele *et al.* (2016) and Hossain *et al.* (2016), while 30% was used for validation. The plots showing the ANN outputs obtained from training and validation are seen in Figure 6. The ANN model very accurately reproduced adsorption capacity and H_2S removal efficiency. A perfect coefficient of determination (R^2) was obtained from the training process. Similarly, the ANN was adequately validated and tested with R^2 values of 0.99 and 0.95, respectively.

The tested and validated ANN model was subsequently employed to predict the adsorption capacity and the H_2S removal efficiency of the Ca-CSAC. The parity plots comparing ANN predicted values of H_2S removal efficiency and adsorption capacity to actual values, from training and validation, are shown in Figure 7. Statistical parameters such as R^2, adjusted R^2 and standard error of estimate were employed to test the validity of the ANN predictions. The ANN predicted values of H_2S removal efficiency are in close agreement with the experimental values for both training and validation data, as seen from the statistical parameters summarized in Table 2. The R^2 value of 1 obtained for the ANN model in both training and validation implies that the H_2S removal efficiency was well fit by this type of model. In other words, the ANN predicted values are statistically reliable. The adjusted R^2 value of 1 signifies that 100% of the data can be explained by the linear model. In both training and validation, the standard error estimate was very low, an indication that the ANN predictive model is reliable with minimal estimation errors. The significance of the ANN predictive model is validated by the p-values below 0.0001 for both training and validation. This further reiterates the robustness of the ANN model to adequately predict the H_2S removal from wastewater.

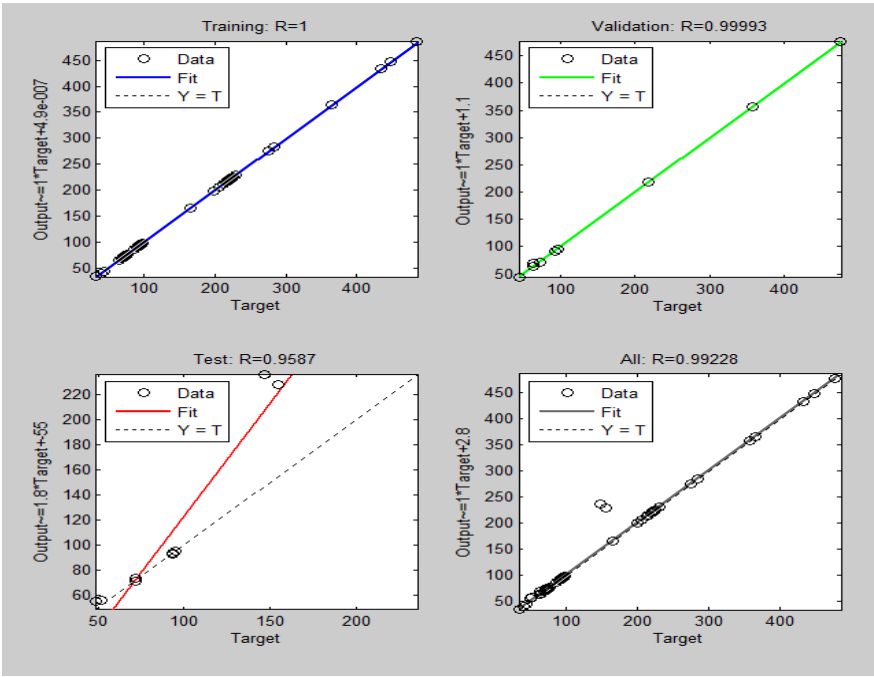

Figure 6. Training and validation of the neural network

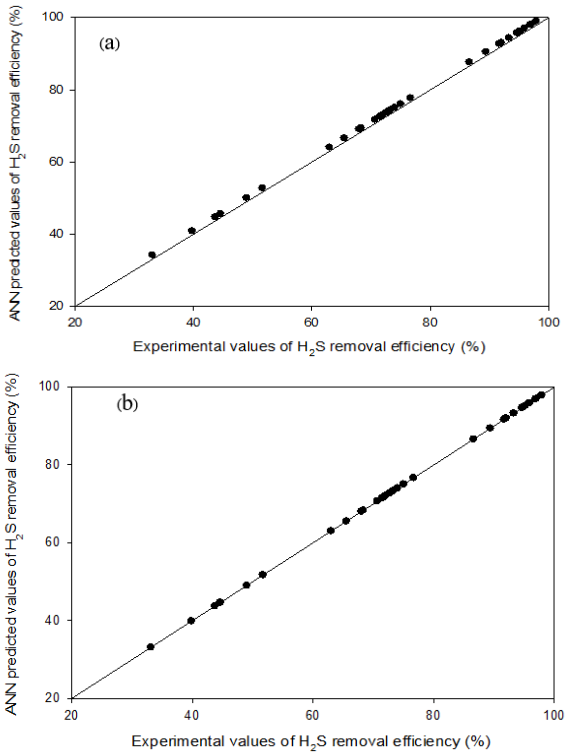

Figure 7. Parity plots showing comparisons between the ANN predicted and the experimental values of H_2S removal efficiency: (a) training, and (b) validation

Table 2. Statistical parameters to assess validity of model fit to H_2S removal efficiency

Statistical parameter	Training	Validation
R^2	1	1
Adj R^2	1	1
Standard error of estimate	$4.32X10^{-14}$	$6.28X10^{-15}$
p-test	<0.0001	<0.0001

Adsorption capacity was also fit with an ANN model subjected to testing and validation. The parity plots comparing ANN predicted values of the Ca-CNSAC adsorption to actual values, for training and validation, are shown in Figure 8. In order to assess the robustness of the predicted ANN values, the statistical parameters R^2, adjusted R^2 and standard error of estimate were employed, as shown in Table 3. Interestingly, the ANN predicted values of adsorption capacity matched experimental values similarly in both training and validation, as seen in the statistical parameters summarized in Table 2. The R^2 values of 1 obtained for the ANN both in training and validation indicate very good model fit by ANN to the experimental adsorption capacity. This is an indication that the ANN predicted values are statistically reliable. The adjusted R^2 value 1 signifies that 100% of the data can be explained by the model. In both training and validation, the standard error of estimate was very low, an indication that the ANN predictive model is reliable with minimal errors. The significance of the ANN predictive model is validated by p-values below 0.0001 in both training and

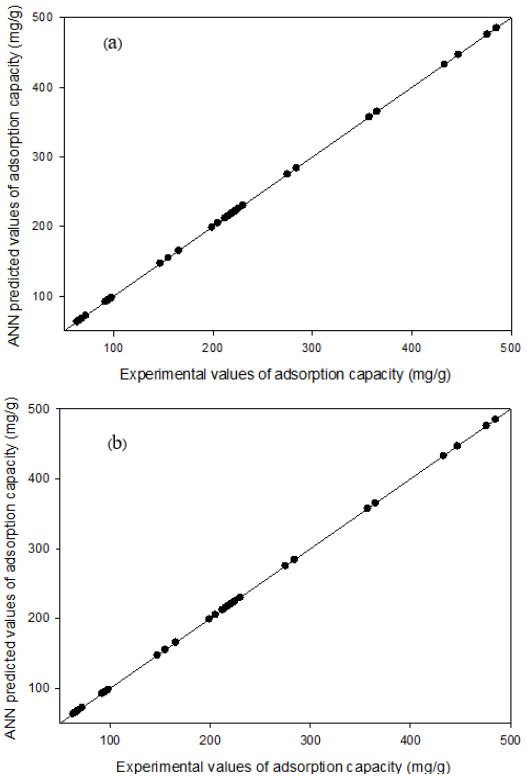

Figure 8. Parity plots showing comparisons between the ANN predicted and experimental values of the adsorption capacity: (a) training, and (b) validation

Table 3. Statistical parameter to assess validity of model fit to predicted adsorption capacity

Statistical parameter	Training	Validation
R^2	1	1
Adj R^2	1	1
Standard error of estimate	$2.44X10^{-14}$	$2.45X10^{-15}$
p-test	<0.0001	<0.0001

validation, which further buttress the adequacy of the ANN model to adequately predict the adsorption capacity of the Ca-CSAC. The accuracy of the ANN model fit for H_2S removal from waste is consistent with the work of Aghav *et al.* (2011), who utilized an ANN for the predictive modelling of competitive adsorption of phenol and resorcinol by wood and rice husk -based activated carbon. The study showed that the ANN perfectly fit the removal efficiency of Phenol and Resorcinol with R^2 values of 0.965 and 0.968, respectively. This predictive performance of the ANN used in this study has demonstrated the capability of ANN models to represent non-linear complex relationships between the input variables and the target variables. In the eventuality of scale-up of the refinery wastewater treatment process using the Ca-CSAC adsorbent, there may exist a non-linear complex relationship between the input and the output variables which needs to be learned from data in order to improve the performance of the process and also to enable predictive control and process optimization.

4. Conclusions

This study confirms the suitability of Ca-coated CSAC as a suitable adsorbent for the removal of H_2S from wastewater. Process parameters such as adsorption contact time, initial H_2S concentration and the Ca-CSAC dosage were found to significantly affect the H_2S removal efficiency and the adsorption capacity of Ca-CSAC. The interactions between adsorption contact time, initial H_2S concentration and Ca-CSAC dosage enabled highest H_2S removal efficiency of 95%. The modeling results showed that ANN is a reliable tool for the prediction of H_2S removal efficiency and adsorption capacity over a range of process conditions. Both training and validation of the predictive models show perfect correlations of model predicted values and actual experimental responses (H_2S removal efficiency and adsorption capacity). The reliability of the ANN as a predictive modeling tool was further assessed through the statistical parameters R^2, adjusted R^2, standard error of estimate, and p-values. The values of 1 obtained for both R^2 and adjusted R^2 confirm that both the predicted ANN values and the experimental values were perfectly correlated. The p-values < 0.0001 and low standard error of estimate obtained for the ANN model show that the ANN has a high degree of reliability for predicting the H_2S removal efficiency and the adsorption capacity. Therefore, with the aid of the predictive ANN model, it will be possible to anticipate and put necessary measures in place that can facilitate the removal of H_2S from wastewater.

References

Adib, F., Bagreev, A., & Bandosz, T. J. (1999). Effect of surface characteristics of wood-based activated carbons on adsorption of hydrogen sulfide. *Journal of Colloid and Interface Science*, *214*(2), 407–415. doi:10.1006/jcis.1999.6200

Agatonovic-Kustrin, S., & Beresford, R. (2000). Basic concepts of artificial neural network (ANN) modeling and its application in pharmaceutical research. *Journal of Pharmaceutical and Biomedical Analysis*, *22*(5), 717–727. doi:10.1016/S0731-7085(99)00272-1

Al-Haddad, A., Azrag, E., & Mukhopadhyay, A. (2014). Treatment experiments for removal of hydrogen sulfide from saline groundwater in Kuwait. *Desalination and Water Treatment*, *52*(16–18), 3312–3327. doi:10.1080/19443994.2013.797544

Asaoka, S., Yamamoto, T., Kondo, S., & Hayakawa, S. (2009a). Removal of hydrogen sulfide using crushed oyster shell from pore water to remediate organically enriched coastal marine sediments. *Bioresource Technology*, *100*(18), 4127–32. doi:10.1016/j.biortech.2009.03.075

Asaoka, S., Yamamoto, T., Kondo, S., & Hayakawa, S. (2009b). Removal of hydrogen sulfide using crushed oyster shell from pore water to remediate organically enriched coastal marine sediments. *Bioresource Technology*, *100*(18), 4127–4132. doi:10.1016/j.biortech.2009.03.075

Ayodele, B. V., & Cheng, C. K. (2015). Modelling and optimization of syngas production from methane dry reforming over ceria-supported cobalt catalyst using artificial neural networks and Box–Behnken design. *Journal of Industrial and Engineering Chemistry*. doi:10.1016/j.jiec.2015.08.021

Ayodele, B. V., Khan, M. R., Nooruddin, S. S., & Cheng, C. K. (2016). Modelling and optimization of syngas production by methane dry reforming over samarium oxide supported cobalt catalyst: response surface methodology and artificial neural networks approach. *Clean Technologies and Environmental Policy*. doi:10.1007/s10098-016-1318-5

Bagreev, A., Rahman, H., & Bandosz, T. J. (2000). Study of H2S adsorption and water regeneration of spent coconut-based activated carbon. *Environmental Science and Technology*, *34*(21), 4587–4592. doi:10.1021/es001150c

Benardos, P. G., & Vosniakos, G. C. (2007). Optimizing feedforward artificial neural network architecture. *Engineering Applications of Artificial Intelligence*, *20*(3), 365–382. doi:10.1016/j.engappai.2006.06.005

Cazetta, A. L., Vargas, A. M. M., Nogami, E. M., Kunita, M. H., Guilherme, M. R., Martins, A. C., . . . Almeida, V. C. (2011). NaOH-activated carbon of high surface area produced from coconut shell: Kinetics and equilibrium studies from the methylene blue adsorption. *Chemical Engineering Journal*, *174*(1), 117–125. doi:10.1016/j.cej.2011.08.058

Cosoli, P., Ferrone, M., Pricl, S., & Fermeglia, M. (2008). Hydrogen sulphide removal from biogas by zeolite adsorption. Part I. GCMC molecular simulations. *Chemical Engineering Journal*, *145*(1), 86–92. doi:10.1016/j.cej.2008.07.034

Dias, J. M., Alvim-Ferraz, M. C. M., Almeida, M. F., Rivera-Utrilla, J., & Sánchez-Polo, M. (2007). Waste materials for activated carbon preparation and its use in aqueous-phase treatment: A review. *Journal of Environmental Management*, *85*(4), 833–846. doi:10.1016/j.jenvman.2007.07.031

Elmawgoud, H. A., Elshiekh, T. M., Khalil, S. A., Alsabagh, A. M., & Tawfik, M. (2015). Modeling of hydrogen sulfide removal from Petroleum production facilities using H2S scavenger. *Egyptian Journal of Petroleum*, *24*(2), 131–137. doi:10.1016/j.ejpe.2015.05.003

Guerrero, L., Montalvo, S., Huiliñir, C., Campos, J. L., Barahona, A., & Borja, R. (2016). Advances in the biological removal of sulphides from aqueous phase in anaerobic processes: A review. *Environmental Reviews*, *24*(1), 84–100. doi:10.1139/er-2015-0046

Guo, J., Luo, Y., Lua, A. C., Chi, R., Chen, Y., Bao, X., & Xiang, S. (2007). Adsorption of hydrogen sulphide (H2S) by activated carbons derived from oil-palm shell. *Carbon*, *45*(2), 330–336. doi:10.1016/j.carbon.2006.09.016

Gupta, V. K., Gupta, B., Rastogi, A., Agarwal, S., & Nayak, A. (2011). A comparative investigation on adsorption performances of mesoporous activated carbon prepared from waste rubber tire and activated carbon for a hazardous azo dye—Acid Blue 113. *Journal of Hazardous Materials*, *186*(1), 891–901. doi:10.1016/j.jhazmat.2010.11.091

Hossain, M. A., Ayodele, B. V., Cheng, C. K., & Khan, M. R. (2016). Artificial neural network modeling of hydrogen-rich syngas production from methane dry reforming over novel Ni/CaFe2O4 catalysts. *International Journal of Hydrogen Energy*. doi:10.1016/j.ijhydene.2016.04.034

Ioannidou, O., & Zabaniotou, A. (2007). Agricultural residues as precursors for activated carbon production—A review. *Renewable and Sustainable Energy Reviews*, *11*(9), 1966–2005. doi:10.1016/j.rser.2006.03.013

Joo, S., Yoon, J., Kim, J., Lee, M., & Yoon, Y. (2015). NO x emissions characteristics of the partially premixed combustion of H2/ CO/CH4 syngas using arti fi cial neural networks. *Applied Thermal Engineering*, *80*, 436–444.

Kastner, J. R., Das, K. C., Buquoi, Q., & Melear, N. D. (2003). Low Temperature Catalytic Oxidation of Hydrogen Sulfide and Methanethiol Using Wood and Coal Fly Ash. *Environmental Science and Technology*, *37*(11), 2568–2574. doi:10.1021/es0259988

Khataee, A., & Khani, A. (2009). Modeling of nitrate adsorption on granular activated carbon (GAC) using artificial neural network (ANN). *International Journal of Chemical Reactor Engineering*. doi:10.2202/1542-6580.1870

Mailler, R., Gasperi, J., Coquet, Y., Derome, C., Buleté, A., Vulliet, E., . . . Rocher, V. (2016). Removal of emerging micropollutants from wastewater by activated carbon adsorption: Experimental study of different activated carbons and factors influencing the adsorption of micropollutants in wastewater. *Journal of Environmental Chemical Engineering*, *4*(1), 1102–1109. doi:10.1016/j.jece.2016.01.018

McBain, J. W. (1932). The sorption of gases and vapours by solids. *The Journal of Physical Chemistry*, *37*(1), 149–150. doi:10.1021/j150343a021

Scott, D. J., Coveney, P. V., Kilner, J. a., Rossiny, J. C. H., & Alford, N. M. N. (2007). Prediction of the functional properties of ceramic materials from composition using artificial neural networks. *Journal of the European Ceramic Society*, *27*(16), 4425–4435. doi:10.1016/j.jeurceramsoc.2007.02.212

Seredych, M., & Bandosz, T. J. (2011). Reactive adsorption of hydrogen sulfide on graphite oxide/Zr(OH)4 composites. *Chemical Engineering Journal*, *166*(3), 1032–1038. doi:10.1016/j.cej.2010.11.096

Silva, P. R., Ponte, H. A., Ponte, M. J. J. S., & Kaminari, N. M. S. (2011). Development of a new electrochemical methodology at carbon steel/Na 2S system for corrosion monitoring in oil refineries. *Journal of Applied Electrochemistry*, *41*(3), 317–320. doi:10.1007/s10800-010-0241-4

Strahand, M. (2010). Removing hydrogen sulphide from water. *Filtration and Separation*, *47*(5), 42–43. doi:10.1016/S0015-1882(10)70215-9

Wang, C., & Pei, Y. (2012). The removal of hydrogen sulfide in solution by ferric and alum water treatment residuals. *Chemosphere*, *88*(10), 1178–1183. doi:10.1016/j.chemosphere.2012.03.065

Wang, X., Jing, X., Wang, F., Ma, Y., Cheng, J., Wang, L., . . . Ning, P. (2016). Coupling catalytic hydrolysis and oxidation on metal-modified activated carbon for HCN removal. *RSC Advances*, *6*(62), 57108–57116. doi:10.1039/C6RA06365A

Xiao, Y., Wang, S., Wu, D., & Yuan, Q. (2008). Experimental and simulation study of hydrogen sulfide adsorption on impregnated activated carbon under anaerobic conditions. *Journal of Hazardous Materials*, *153*(3), 1193–1200. doi:10.1016/j.jhazmat.2007.09.081

Zamaniyan, A., Joda, F., Behroozsarand, A., & Ebrahimi, H. (2013). Application of artificial neural networks (ANN) for modeling of industrial hydrogen plant. *International Journal of Hydrogen Energy*, *38*(15), 6289–6297. doi:10.1016/j.ijhydene.2013.02.136